

We are IntechOpen, the world's leading publisher of Open Access books Built by scientists, for scientists

4,800

Open access books available

122,000

International authors and editors

135M

Downloads

Our authors are among the

154

Countries delivered to

TOP 1%

most cited scientists

12.2%

Contributors from top 500 universities

**WEB OF SCIENCE™**Selection of our books indexed in the Book Citation Index
in Web of Science™ Core Collection (BKCI)

Interested in publishing with us? Contact book.department@intechopen.com

Numbers displayed above are based on latest data collected.

For more information visit www.intechopen.com

Powered Human Gait Assistance

Kevin W. Hollander* and Thomas G. Sugar†

*Augsburger-Komm Engineering, Inc., Phoenix, Arizona

†Arizona State University, Mesa, Arizona

USA

1. Introduction

Wearable robots are computer-controlled, actuated devices that are worn by a person. The purpose of such a device is to enhance the strength or performance of the person that wears it, where performance can be speed or coordination or some other desired attribute. Potential uses of a wearable robot are in rehabilitation, training, strength augmentation or simply as an assistance device for normal daily living. The greatest potential impact that a wearable robot could have is in the rehabilitation or assistance of a weak or disabled person.

Within the growing elderly population, 20 to 50% are affected by abnormal gait, i.e. walking impairment (Rubenstein & Trueblood, 2004). Abnormal gait in the elderly does not have a specific cause; many age related factors can affect normal locomotion. Some examples include; 1) muscle weakness, 2) slow reaction times, and 3) impaired tactile sensation from the feet. The ability to balance is the first requirement for successful gait. Impaired sensory information, long processing times and weak actuation all lead eventually to an unstable balance control system.

Adaptation of powered actuated devices to assist elderly or weak individuals implies special design requirements (Hollander & Sugar, 2004). Use of the term 'wearable' implies that such a robot be portable, lightweight and safe. In order for such a device to be accessible for home use, the additional implications are that the wearable robot be economical and easy to operate. In contrast, a factory floor robot is none of these things; therefore, simple adaptation of existing technology is not possible.

The goal of this work is to investigate these design requirements and to develop the methodologies necessary for their implementation to human gait assistance. This work will focus on the use of a novel spring based actuator, which is powerful, lightweight, energy efficient and above all safe to its wearer.

2. Background

The prevalence of powered assistance devices for the weak and elderly can be seen almost every day. Powered-seated scooters are increasingly popular and are available from a variety of commercial sources. Often these scooters require additional modifications to one's home and automobile to accommodate their use. The popularity of the seated scooter is testament to the need for powered assistance; however, the use of these devices are in direct conflict to the belief that long term health is maintained by the inclusion of "the types of

Source: Rehabilitation Robotics, Book edited by Sashi S Kommu,

ISBN 978-3-902613-04-2, pp.648, August 2007, Itech Education and Publishing, Vienna, Austria

activities that provide an adequate load-bearing stimulus" (ACSM, 1995). Powered assistance is required, but should come in a form that promotes and supports standing/walking activities. To maintain general health and wellbeing, load-bearing walking is essential.

However, the solution to developing a walking assistance robot is not trivial. It is well known that such a system would need the ability to produce large torques and be capable of high power. Such requirements raise the threshold for wearable robots to be successful in this application. Nevertheless, work in this area has already begun.

Projects in the area of assisted locomotion are the BLEEX (Berkeley Lower Extremity Exoskeleton) robot (Kazerooni et al., 2006) and the HAL-3 (Hybrid Assistive Leg) robot (Kawamoto et al., 2003; Kawamoto & Sankai, 2002). Both devices are rigidly attached to the wearer and are directly driven, i.e. no compliant interface.

The BLEEX robot uses hybrid hydraulic actuators to drive the system, whereas the HAL-3 robot uses DC motors and gearboxes to provide power for movement to the user. In both projects, the same solution is used, providing both positive and negative forces to the user to achieve a desired movement pattern. For example in gait, sometimes the robot needs to push the user (positive) and sometimes for support the robot needs to resist the user (negative) and in either case the robot is putting power into the system.

In other work, a robotic powered knee, RoboKnee (Pratt et al., 2004), and an active ankle foot orthosis, AAFO (Blaya & Herr, 2004) have been developed to assist with an individual's gait. Each of these devices features the linear Series Elastic Actuator (Robinson et al., 1999) as the means of robotic control. The linear series elastic actuator features a helical spring in series with a ball screw mechanism, similar to the actuator developed by Sugar and Kumar (Sugar & Kumar, 1998) for grasping tasks. For the series elastic device, the inclusion of the spring aids greatly in force and impedance control task stability. However, even though the device uses a spring between the actuator and the environment (i.e. person), the compliance of this system is derived mostly from its controller. Based upon the geometry and length of the springs used, very little deflection or compliance would be possible in a passive situation and thus is still very nearly a directly driven system.

Common knowledge in the legged robot community is that inclusion of springs in robotics can effectively reduce both the power and energy requirements demanded of an actuator (Raibert, 1986; Hurst et al., 2004). This is because a spring can store and release energy efficiently during cyclic repetitive tasks and the power released from a spring is limited only by the natural frequency and stiffness of the system. In other literature, van den Bogert describes a theoretical, passive mechanism that reduces peak power for human gait by more than 70% (van den Bogert, 2003). The passive device uses a series of elastic cords and pulleys around multiple anatomical joints to accomplish reduced power requirements. As written, the specific implementation described would not likely be practical, but the point of including springs in the design of wearable robotic systems is beneficial.

In order to meet the demanding requirements stated above, a wearable robotic device must include lightweight, energy conservative, power reducing springs to be both portable and inherently safe.

3. Human Ankle Gait

A basic understanding of human ankle gait is required before a discussion of actuator strategies for ankle gait assistance can begin. Gait is the term used to describe the

locomotion of legged animals. Gait is a reoccurring pattern of leg and foot movements, rotations, and torques. The discussion of gait is presented in terms of percentages of a gait cycle due to its repetitive nature. The basic description of gait analysis terms is illustrated in figure 1.

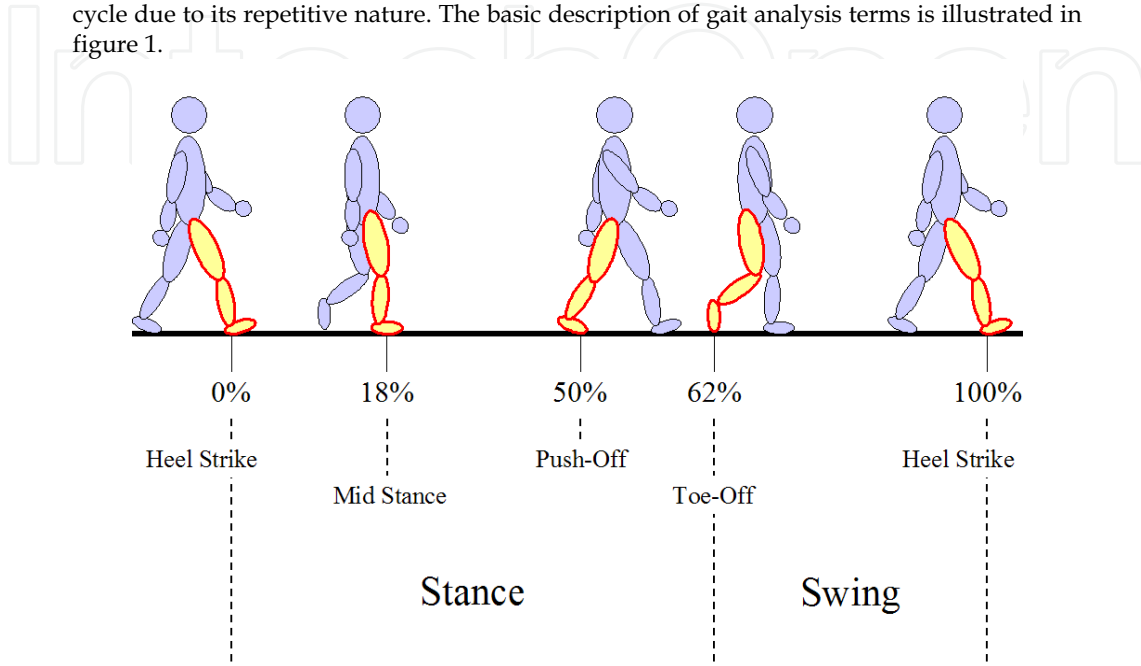


Fig. 1. Normal Gait Cycle.

As can be seen in the figure, a gait cycle is defined for a single leg and begins with the initial contact of the foot with the ground or 'heel strike'. The conclusion of a cycle occurs as the same foot makes a second 'heel strike'. The end of one gait cycle is of course the beginning of another.

Other key regions of the gait cycle are indicated in figure 1 as mid stance, push-off, and toe-off. In this case, the mid stance is shown with the leg perpendicular to the foot at the ankle. At this point in the gait cycle the body's weight is aligned over the primary supporting foot. The peak thrust of the push-off phase of gait is diagrammed at 50% of the gait cycle. Push-off is the propulsive phase of gait, giving the body its continued forward motion. The toe-off event begins at the completion of push-off, which is the beginning of leg swing. At toe-off, the hip is fully extended and the leg and foot are advanced to prepare for the next step or heel strike. To illustrate a typical pattern of gait, consider the kinematics and kinetics of a normal ankle (Whittle, 1996), figure 2; notice that the ankle moment (torque) data is normalized by body weight (kg).

In this figure, peak ankle moment occurs at roughly 45% of the gait cycle and at a value of -1.25 Nm/kg or for an 80 kg person, -100 Nm . The negative sign represents the physiological direction for which the moment occurs. In this case, peak moment is acting to move the foot in a toes-down direction. Interesting to note, the point at which the peak moment occurs, the ankle angle begins a rapid descent to its lowest overall value of -24° at 60% of the gait cycle. The region of gait approximately between 40% and 60% of the gait cycle is known as 'push off' (highlighted on each plot).

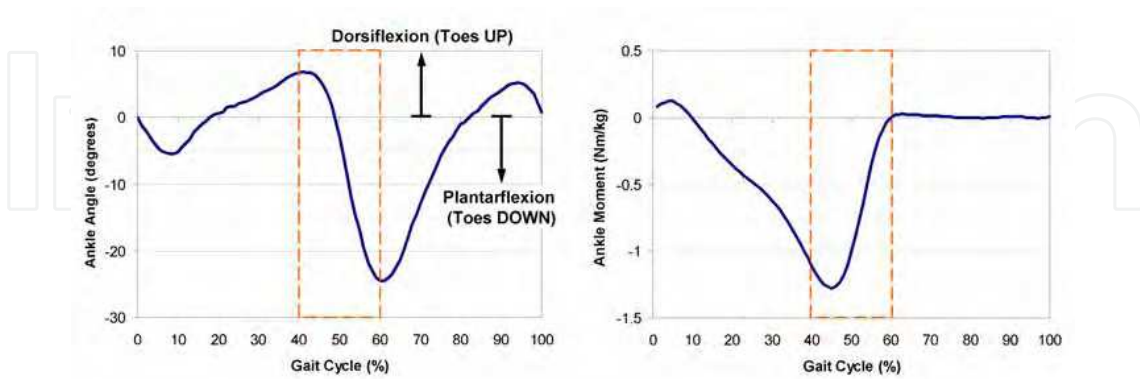


Fig. 2. Normal Ankle Gait: Kinematics and Kinetics.

This data provides information about the torques and angles required to achieve normal ankle gait. In terms of an actuator, these torques and angles can be converted into required forces and displacements. An actuator following this linear data will provide normal gait. Knowing the forces and positions necessary for gait is the first step. The next step is to determine the power requirements, which is used to size the motor for this task.

In order to determine the power of gait for the human ankle, it is necessary to assume a person's body weight and gait speed. This information, combined with the data for normal ankle gait, i.e. figure 2, are used to calculate ankle power for an ideal person who weighs 80 kg and walks at a frequency of 0.8 Hz, see figure 3.

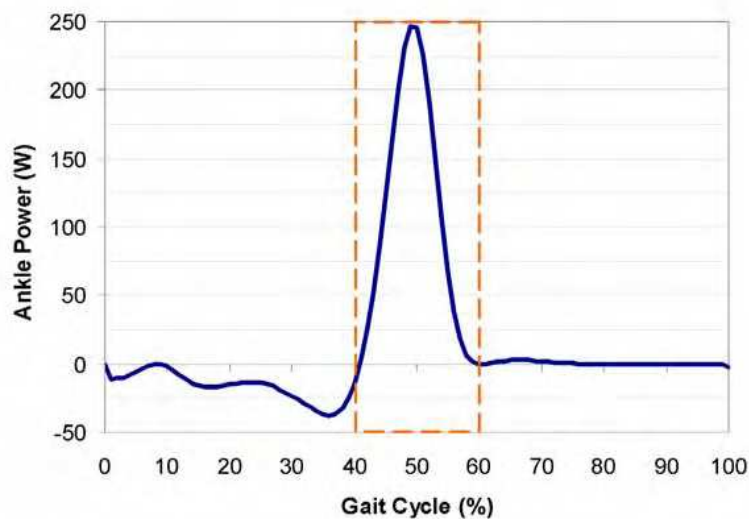


Fig. 3. Normal Ankle Gait Power, 80 kg person, 0.8 Hz gait frequency.

Notice that the ankle requires primarily positive power for the task of 'push off' (i.e. 40%-60%). For most of the ankle's power needs the requirements are modest, but during the

push off phase of gait it spikes to 250 W. Considering both the negative and positive portions of power, average power for this task is only 15 W. The power required during the swing phase of gait is minimal because little torque is needed to reposition the foot for the next heel strike. An integration of the power curve yields a total value of energy for each ankle to be 19.4 Joules/step.

Additionally, the primary source for this peak power or propulsion in normal gait is the gastrocnemius and soleus muscle groups. These muscle groups are located at on the backside of the lower leg and are often referred to as the calf muscles. Flexing these muscles produces a downward thrust of the foot or plantar flexion moment about the ankle. Experimental recordings of muscle activity are achieved via electromyography or EMG instrumentation. During a muscular contraction, positively charged calcium ions flow within the muscular tissue. The movement of these charged particles creates a change, or flux, in the magnetic field surrounding the muscles, and can be captured or measured by electromagnetically sensitive equipment, i.e. EMG electrodes.

Once captured, an EMG signal can be processed and observed. For the gastrocnemius muscle group, a rectified and processed EMG signal is shown for normal gait, see figure 4 (Hof et al., 2002).

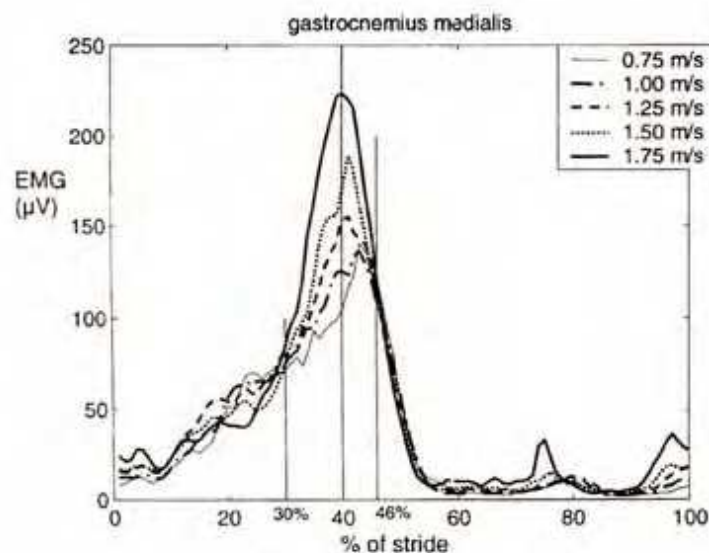


Fig. 4. Normal Ankle Gait EMG: Gastrocnemius Muscle Group (reprinted with permission from Hof et al., 2002).

Figure 4 shows several processed EMG signals, each for a different gait speed. Logically, the data shows higher amplitudes in muscular response for increases in gait speed. The raw signals for this data have been filtered for noise, rectified and enveloped as part of the processing. The result is the relatively clean looking signals displayed in the figure. EMG signal measurements are sensitive to many factors and thus its amplitude can be compared only under carefully considered situations.

For example, in the displayed data, the measurements were recorded sequentially during the same testing session. In this case, it is appropriate to compare the amplitudes of these signals. However, these same amplitudes have no real meaning for comparison to another subject or even the same subject on a different day. As such, the real usefulness of an EMG measure is in capturing the relative shape and timing of muscular activity and not its amplitude. From figure 4 it is apparent that peak amplitude of EMG activity of the gastrocnemius occurs just prior to the push-off phase of gait. In a later section, the significance of this shape and timing will be discussed.

4. Robotic Tendon Approach

The Robotic Tendon is the name given to our spring-based actuator (Hollander et al., 2006b). Use of the term Robotic Tendon implies an analogy to human physiology. The premise of the following development is that the human muscular system uses the advantages inherent in its elastic nature. Therefore, similar to a human muscle, the elastic nature of a spring is used to minimize both the work and peak power required to perform the task of ankle gait. A conceptual model of the Robotic Tendon can be seen in Figure 5. Conceptually, this model is same model described by Sugar and Kumar (Sugar & Kumar, 1998; Sugar, 2002) as well as the linear series elastic model described by Robinson (Robinson et al., 1999).

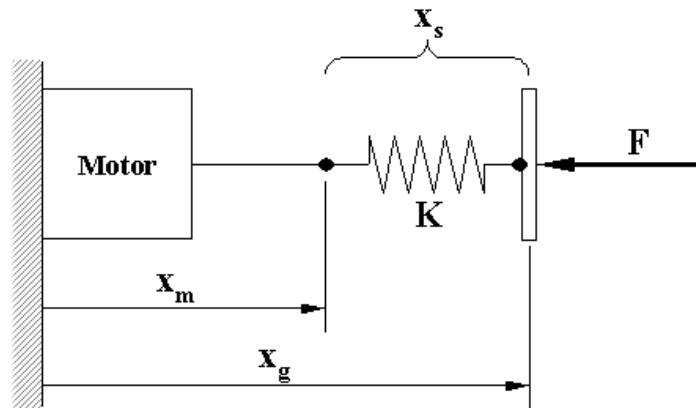


Fig. 5. Robotic Tendon Model: motor and spring in series.

From figure 5, a development of motor power requirements based upon stiffness K can be derived. The position of the environment, x_g , is given by converting the joint angles of gait to linear displacement using a simple lever arm. In the model, the position, the compression of the spring and the movement of the motor can achieve x_g . It is thus a combination of the position of the motor, x_m , and the position of the spring, x_s , see equation 1.

$$x_g = x_m + x_s \quad (1)$$

However, since a spring is a passive device its position is determined by the force, F , applied to it. The force, F , is calculated by converting the moment needed in gait using a simple lever arm. Consider the basic Hookean spring shown in equation 2.

$$F = K \cdot \Delta x_s \quad (2)$$

where, $\Delta x_s = d_o - x_s$.

The free un-deformed length of the spring is represented by d_o and is simply an offset value. Solving equation 2 for x_s , yields:

$$x_s = d_o - \frac{F}{K} \quad (3)$$

The length of the spring is based upon the environmental force and spring stiffness. Equation 3 can be substituted into the equation for environmental position, x_g , and solved for the required motor position, x_m . From this substitution equation 4 is determined,

$$x_m = x_g + \frac{F}{K} - d_o \quad (4)$$

and taking its derivative, yields the velocity required.

$$\dot{x}_m = \dot{x}_g + \frac{\dot{F}}{K} \quad (5)$$

Knowing the forces, F , required by the gait cycle and knowing the motor's required velocity, \dot{x}_m , the relationship for motor power, P_m , can be obtained. Power is simply force multiplied by velocity, thus multiplying F by equation 5 will yield a relationship for motor power.

$$P_m = \left| \underbrace{F \cdot \dot{x}_g}_{\text{required gait power}} + \underbrace{\frac{F \cdot \dot{F}}{K}}_{\text{spring power}} \right| \quad (6)$$

Human ankle gait power can be both negative and positive. When it is negative, a resistance motion is applied to the ankle, and when it is positive, a propelling motion is applied. A motor unit cannot typically provide negative power; therefore, it must provide power to both resist and propel human motion. For this reason, an absolute value in equation 6 is used. In addition, values for force, F , velocity, \dot{x}_m and \dot{F} can all be determined from human gait analysis data. Thus, stiffness, K , becomes the only design parameter.

Consider the case where spring stiffness, K , is nearly infinite (i.e. direct drive). In this example the spring power term drops to zero and the motor must provide the absolute value of normal gait power. In the opposite case, consider a spring with stiffness near zero. In this example, the power requirements tend toward infinity. If a straight line were assumed between these two cases, it would appear that a direct drive scenario is the best.

Fortunately, this simplistic relationship is not the case. On the contrary, if a spring is properly selected both energy and peak power for the motor required to perform human gait can be drastically reduced compared to the direct drive analogy.

4.1 Stiffness for Zero Motor Power at Peak Output

As a first approach to determining stiffness, consider the form of equation 6. In terms of a design, the only variable to pick is spring stiffness. The rest of the terms in this equation are

dictated by ankle gait kinematics and kinetics. So, what is the best method for choosing stiffness?

One possibility is to try and minimize the motor's power demand during the most demanding portion of the gait cycle. If the peak motor requirement could be driven lower than 247 W described earlier, then a smaller and thus lighter motor could be chosen for the actuator. So as a first approach, equation 6 can be set equal to zero and solved for K.

$$K = \frac{\dot{F}}{\dot{x}_g} \quad (7)$$

Evaluating equation 7 for the example gait data, using a 0.12 m lever arm, yields a stiffness $K_1 = 14,152$ N/m. The peak power of gait occurs at 50% of the gait cycle. Using this calculated value of stiffness, power of the motor will equal zero during the peak power of gait. Initially, this may seem counter intuitive, but consider that a spring can store energy over time and yet release it very quickly (i.e. high power). In the case of the Robotic Tendon, at this stiffness, the spring is providing 100% of the power needed for gait at the instance of peak demand. Figure 6 shows the power profile that results from choosing this stiffness.

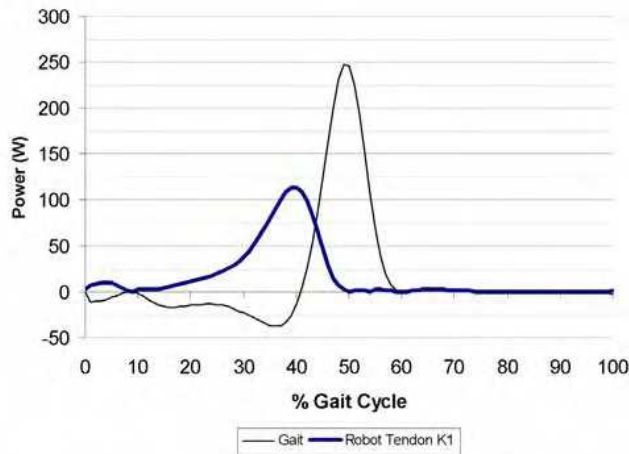


Fig. 6. Robotic Tendon Power with $K_1 = 14,152$ N/m: Zero motor power at peak gait power.

The figure shows a thick line for the Robotic Tendon power and a thin line for the power required for ankle gait. The resulting power curve for the Robotic Tendon differs significantly from the one developed for a lead screw only or direct drive actuator. In this case, the ankle gait curve and motor curve do not seem to match. The difference between these two curves is the addition of the spring power. The addition of spring power to the motor power will result in the appropriate ankle gait output.

Noteworthy in this graph is the much lower value of peak power for the motor compared to ankle gait. Even with the addition of efficiency of the lead screw, a motor sized below 150 W can easily perform this gait task. As an example, the Maxon RE40 DC motor is nominally rated for 150 W of continuous power and weighs only 0.48 kg. With a small 6 mm diameter lead screw design, the combined weight of the K_1 actuator is still less than 1 kg and would

consume only about 23 J per step. This provides a much better result than the lead screw only actuator, which would require a much larger motor and thus a heavier design.

Consider again the analogy of the Robotic Tendon to human muscle and its response to the task of ankle gait. Previously, figure 4 showed the timing and shape of the EMG response of gastrocnemius muscle during gait. EMG has often been correlated to muscular force. However, consider the shape and timing of the motor power curve for the Robotic Tendon compared to EMG signal of the gastrocnemius. Both of these actuators are performing a similar function and both use elasticity to minimize power and to conserve energy. For convenience, a scaled plot of both of these figures was constructed, see figure 7.

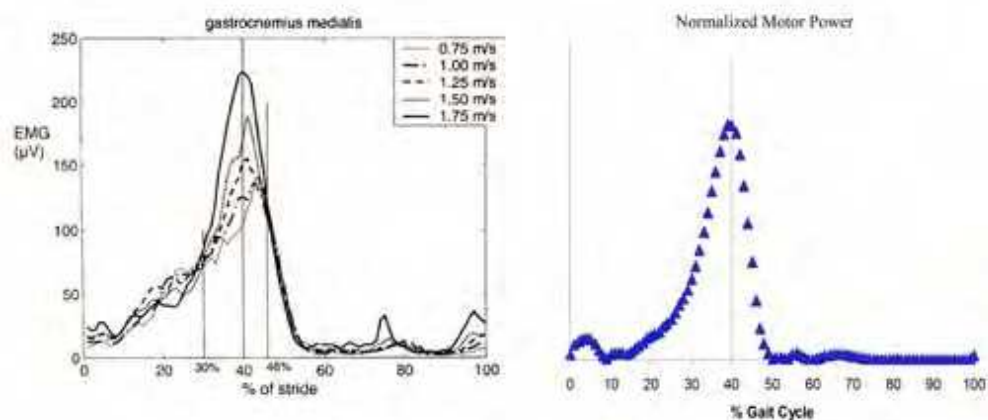


Fig. 7. Robotic Tendon Power and EMG Comparison: Triangles represent the calculated Robotic Tendon power data, scaled to fit the previously referenced EMG data plot of the gastrocnemius muscle group (reprinted with permission from Hof et al., 2002).

The magnitudes for these sets of plots have no meaning in the present comparison. Only the shape and timing need to be considered. It is remarkable to see the level of similarity between the two sets of plots. Although this is not a conclusive result, it is nonetheless a strong indication of relationships. If EMG is more closely related to power of the muscle than force, it is still not surprising to see that an EMG/force correlation would exist. Consider that power is defined as force multiplied by velocity and so EMG and power would each follow force closely. The significance of these similar graphs is that the models of a Robotic Tendon could provide a clean and simple explanation as to how the human uses his own muscle motors. This topic is a separate discussion to the present analysis, but still offers an interesting result to share.

4.2 Stiffness Optimization

Using the above method for selecting stiffness yields good results for the Robotic Tendon actuator. These results may even indicate that the human's gastrocnemius muscle group could be using a similar strategy. If this is the case, can a better result be obtained? To answer this question an exploration of the influence of stiffness, K , on peak motor power is required. Based upon equation 6, the relationship between stiffness, K , and 'peak' motor power is considered in equation 8.

$$(P_m)_{peak} = \max \left| F \cdot \dot{x}_g + \frac{F \cdot \dot{F}}{K} \right| \quad (8)$$

To run the optimization, a C++ program was written to calculate the maximum motor power during a gait cycle for a large range of spring stiffness values. The code was run for several iterations to further refine the optimization results. To explain these results, a plot of only peak motor power was produced for a successive range of spring stiffness's. This plot can be seen in figure 8.

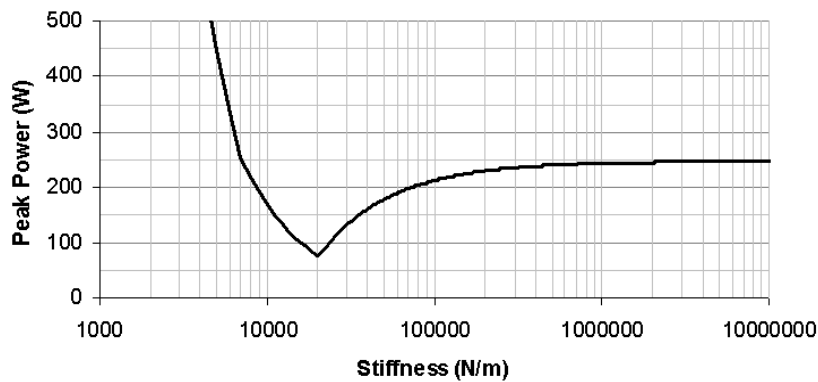


Fig. 8. Optimization of Stiffness, K , for an 80kg person.

Figure 8 reveals an interesting relationship. Extreme stiffness cases can be described by this graph and its corresponding equation. At a stiffness value near zero, infinite motor power would be required. The analogy is that the spring is absorbing all of the power that the motor can provide and is not providing any back to the environment. At the opposite extreme is infinite stiffness or direct drive (i.e. lead screw only design). It is seen that a high stiffness spring asymptotically approaches peak gait power near 250 W. However, rather than being a linear relationship between the two extremes, a minimum point or cusp occurs. The odd shape of this graph can be explained as follows. The driving profile for this plot is determined by a $-1/K$ relationship with respect to power. The cusp is created as a function of the absolute value of this factor and hence a minimum is created. For the example problem, an optimal value of stiffness, K_2 , is determined to be 20,278 N/m. Figure 9 shows the power profile that results from choosing this new stiffness.

The figure shows a thick line for the Robotic Tendon power and a thin line for the power required for ankle gait. The resulting power curve for the Robotic Tendon is very different from the one developed for a lead screw only actuator and is different still from the previous stiffness choice. The peak power for the motor using this stiffness is lower than was seen in the previous stiffness case. Including the effects of friction on this graph, a motor sized below 90 W can be used. As an example, the Maxon RE35 DC motor is nominally rated for 90 W of continuous power and weighs only 0.34 kg, that is 30% less weight than in the previous example. Again, considering the effects of friction, the K_2 actuator would still consume only about 23 J per step. Even though the power results have been improved between the K_1 and K_2 stiffness cases, the energy of either approach is the same.

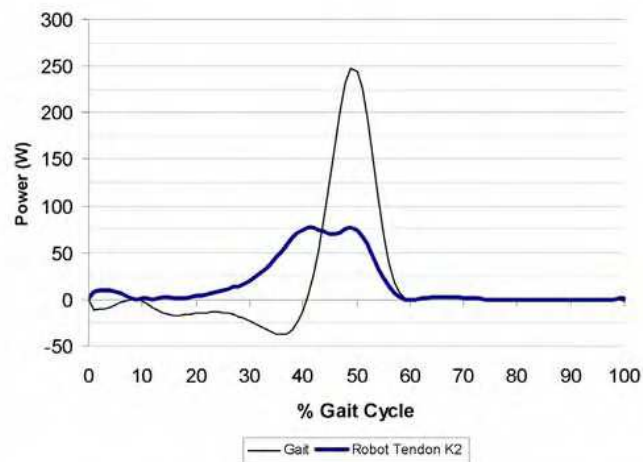


Fig. 9. Robotic Tendon Power with $K_2 = 20,278 \text{ N/m}$: Optimized stiffness.

4.3 Experimental Results

The Robotic Tendon actuator just described was used on a volunteer subject. As an additional means of safety during early testing, the ankle gait actuator was not allowed to drive the subject's ankle joint. Instead, the subject's foot was placed into a rigid and locked orthosis and the robot manipulated the position of its own separate ankle.

In this first prototype it was useful to separate the function of the robot from the function of the human ankle. This separation allows a clean comparison of results from the robot to the functional predicted expectations presented above. Had the robot been used to only assist in moving the subject's true joint, obtained results would not clearly separate the power supplied by the person from that of the robot.

For this experimental work, the subject tested was not the same size as our ideal subject.

Our ideal assumptions were developed for a typical young adult male, 80 kg. Our subject was slightly smaller and weighed just 65 kg. The significance of this difference is that the previously selected stiffness of $K = 20,278 \text{ N/m}$ would not be the optimal result for the tested subject. Nevertheless, using the same formulation as above, the response of the robot can still be predicted for this alternative set of conditions. In the following graphs, Figure 10, the predicted and measured positions of both the robot's end effector (lever) and the motor nut are presented.

The end effector position is the physical position of the forward end of the spring, i.e. the point at which the robot foot is attached. The motor nut position is the linear displacement of the nut along the lead screw; this is also coincident with the back end of the spring. Looking first at figure 10A, the thin line represents the end effector path through the gait cycle. The thick line in this plot represents the path of the motor nut. The difference between these lines is the deflection of the spring.

Comparing figure 10A with 10B reveals a very similar set of results. In general the measured data in figure 10B does not get the range of motion predicted, but still manages to get significant deflection of the spring. These results are quite remarkable in light of the fact that the only control variable for the robot was to maintain the thick lined path seen in figure

10B. The thin line in this plot was generated completely by the subject walking on the robot. This shows that the natural response of the human is to use the elastic compression spring similar to how his own elastic musculotendon complex would be used in gait. In a separate trial of data collection, the force and power profiles measured by the actuator were obtained. The results of these measurements are shown once again in comparison to predicted values, see figure 11.

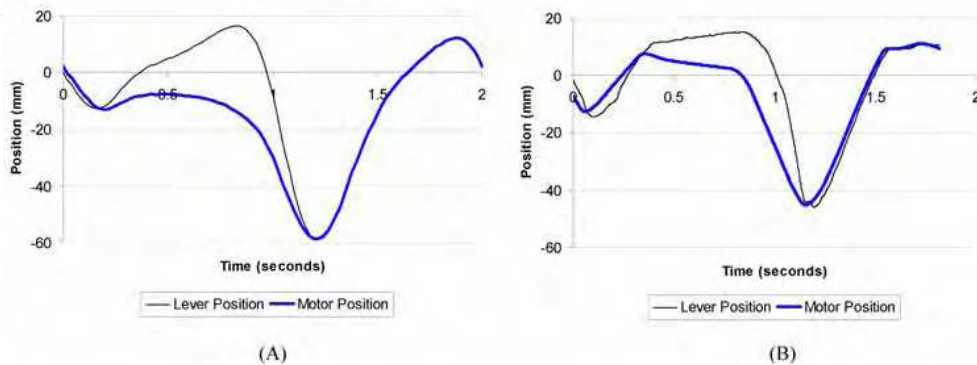


Fig. 10. Robotic Tendon Experimental Results: Position, A) Predicted results of end effector (lever) and motor nut positions, B) Measured results of the same.

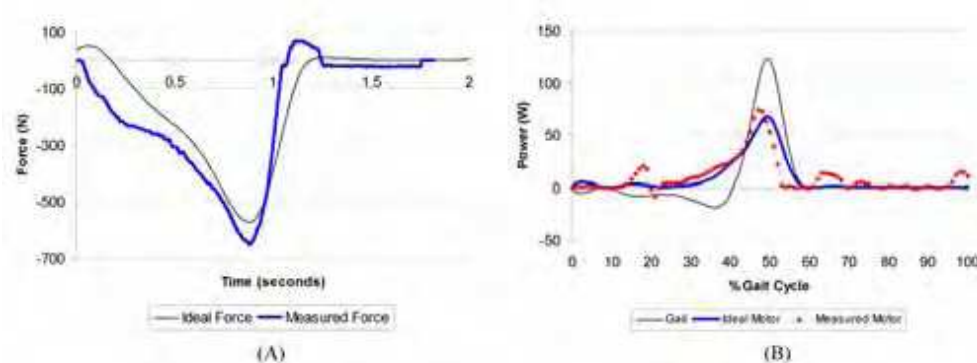


Fig. 11. Robotic Tendon Experimental Results: A) Forces and B) Powers.

Again for both graphs the predicted and experimental results match very well. In figure 11A, the measured force is shown to slightly exceed predicted (ideal) and it descends to zero more rapidly from its peak. Figure 11B, shows a similar result for power as seen in force, a slightly higher peak is reached but drops to zero earlier in time. The result of power is shown with its ordinate axis as a percentage of a gait cycle, while forces were shown in seconds. During testing and comparisons, gait frequency was reduced to a just 0.5 Hz, for added safety.

In recent work, a 50% assistance ankle robot was constructed. Figure 12 shows this robot. The robot features a rear-mounted actuator that allows the user to easily don and doff the device. The Robotic Tendon actuator is tuned to provide 50% assistance to the wearer.



Fig. 12. Robotic Tendon prototype.

5. Application to Elderly Gait

Muscle weakness, slow reaction times, and impaired tactile or sensory information from the feet can affect a person's ability to balance and thus affect their ability to walk. For the complex tasks of balance and gait, significant deficiency in any of these factors pushes the limits of postural stability to 'marginal' at best. The result of these factors is an increase in duration of double-limb support during gait, which leads to a decrease in walking speed.

This decrease in elderly gait is approximately 12-20% less than the speed of a typical young adult (Elble, 1997; Winter, 1991). It is interesting to note is that this decrease in speed is not due to a reduction in cadence (i.e. frequency of gait), but is attributed to a decrease in stride length, or reach. The term 'cautious gait', coined by Nutt et al. (Nutt et al., 1993), describes this phenomenon as the response to a "real or perceived disequilibrium". Cautious gait is the result of apprehension to falling.

A wearable robot device can potentially aid in these difficulties. A wearable robot would provide strength where there is weakness, respond to stimuli quickly rather than slowly, and a wearable robot would sense problems early, rather than after it is too late. To assist elderly gait, a wearable robot based upon the idea of the Robotic Tendon actuator can be created.

The gait kinematics and kinetics for an elderly individual are different than for a younger able-bodied person. A shorter stride length, an increase in double stance time and ultimately a decrease in ankle power production are all hallmark characteristics of elderly gait (Winter, 1991; Devita & Hortobagyi, 2000). The gait kinematics and kinetics for an elderly individual (Devita & Hortobagyi, 2000) can be seen in Figure 13.

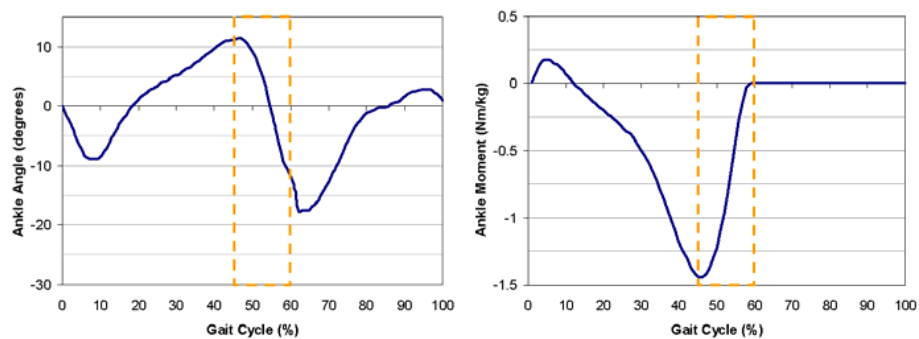


Fig. 13. Elderly Ankle Gait: Kinematics and Kinetics.

Different from the young able-bodied gait data, the elderly ankle gait kinematics has increased ankle dorsiflexion and reduced plantarflexion. Although the peak moments still occur roughly at 45% like young able-bodied gait, the peak moment is slightly greater. At a value of -1.44 Nm/kg the peak moment for an 80 kg person is -115 Nm . Also, the 'push off' phase of elderly gait starts about 5% later than for young able-bodied gait and ranges from roughly 45% to 60% of the gait cycle (again highlighted on each plot).

In order to determine the power of elderly ankle gait, it is necessary to assume body weight and gait speed. Using the elderly ankle gait kinematics and kinetics presented in Figure 13, ankle gait power can be calculated for 80 kg individual that walks at a frequency of 0.8 Hz, see figure 14.

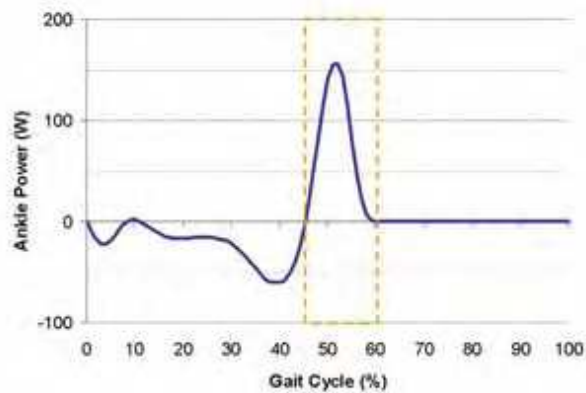


Fig. 14. Elderly Ankle Gait Power, 80 kg person, 0.8 Hz gait frequency.

Elderly ankle gait power has a lower positive peak power than does young able-bodied gait, 157 W compared to 250 W. Also, integration of the power curve yields a net energy of just 1.5 Joules/step. This is much less energy than is calculated for young able-bodied gait (19.5 Joules/step). A slightly greater amount negative peak power and 5% longer time allows an elderly ankle to store additional energy into its elastic structures. This combined with lower a positive peak power yields a very low combined or net positive energy added during each step.

Just like in the able-bodied Robotic Tendon actuator development, optimal spring stiffness can be chosen to reduce actuator motor peak power requirements for elderly gait and thus provide a very lightweight actuator design. A power optimization analysis for an 80 kg elderly individual, using a 0.12 m lever arm, yielded an ideal stiffness of $K_3=29,929$ N/m. The effect on the power input and output can be seen in Figure 15.

The figure shows a thick line for the Robotic Tendon power and a thin line for the power required for ankle gait. The peak power for the motor using this K_3 stiffness is less than 40 W. As an example, the Maxon RE30 DC motor is nominally rated for 60 W of continuous power and weighs only 0.238 kg. The RE30 motor weighs only half of the weight of the RE40 motor mentioned earlier. Motor energy calculated for this elderly gait assistance design is only about 12 Joules/step.

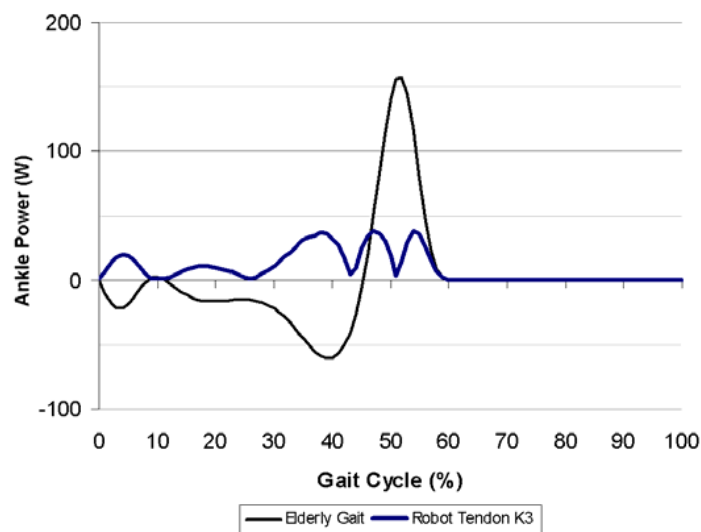


Fig. 15. Elderly Ankle Gait, Robotic Tendon Power with $K_3 = 29,929$ N/m.

Providing correctly timed energy and power to an elderly individual's gait is the first step to assistance. It may be that powered gait assistance for the elderly must come in the form of the elderly gait pattern shown. However, if appropriate strength and timing is given to such a person, then maybe powered assistance can restore a young able-bodied gait profile to that elderly individual. Additional work in this area is still needed. The extent of influence such powered assistance has on elderly gait or even, pathological gait is simply not yet known.

6. Application to Hips and Knees

As seen in the previous development, the Robotic Tendon approach can be applied to alternative patterns of gait. In fact, the same method can be adapted to develop power-minimizing actuators for other joints, like the knees or hips. A Robotic Tendon actuator can be designed for any anatomical joint and provide a compliant, robust, powered assistance for a variety human movements. However, in order for a Robotic Tendon actuator to be designed to significantly minimize required motor power, special movement characteristics must exist.

As an example, the reason the Robotic Tendon approach successfully reduces motor power for the task of ankle gait is due to the nature of output movement of the ankle. Ankle gait patterns are asymmetrical in terms of power output. Relatively speaking, ankle power requirements are low and absorptive for the majority of the gait cycle and then during 'push off' energy is released very quickly (high power).

In contrast, hip gait motion is much more symmetrical and as a result only minimal power savings are achieved by optimizing the spring stiffness. For the same 80 kg individual, walking at a 0.8 Hz rate the peak hip output power is 82 W. An optimization of the spring for hip gait assistance yields a stiffness value of 16,970 N/m. A Robotic Tendon actuator tuned for this stiffness would require a motor peak power value of just 60 W. In this example, the power savings is only on the order of 27%. Even considering only modest savings in peak power required, use of a spring-based actuator for powered hip assistance is still recommended. A spring is a compliant and an efficient form of energy storage, and thus will provide a good basis for most wearable robot designs.

Different from the hip and the ankle, knee power requirements for gait shows that the mean output is negative and the peak magnitude is around -80 W. With a majority of the output power requirements being negative, controlled damping (energy dissipation) can provide a good assistance solution. Examples of devices that control damping at the knee are the Rheo Knee (Ossur, Iceland) and the C-Leg (Otto Bock Healthcare, Germany) prosthetic knee devices.

A Robotic Tendon actuator can also provide controlled damping utilizing its spring. Mentioned previously, using a spring is an efficient method of energy storage. However, since the motor is used to control the backside of the spring, this stored energy does not have to be completely returned to the environment. Imagine compressing a spring from one side and then allowing backside of the spring to slowly release that stored energy. Motorized control of a spring's total deflection is the fundamental nature of the Robotic Tendon approach.

Although the knee power profile is primarily negative, it still requires some positive power contribution. The Rheo Knee and C-Leg do not provide this additional required energy. A spring-based actuator can add, subtract or even store energy as needed and thus provide full powered walking assistance at the knees.

7. Control Methodology

Conceptually, the control approach used for the Robotic Tendon is an approach called 'equilibrium control' (Hollander & Sugar, 2004). A linear actuator is used to drive the backside of the spring, effectively moving the un-deflected or equilibrium position of the spring. The basic premise of this approach is to position the spring into the right place, at the right time, so that the device operator (wearer) can take advantage of its elastic properties.

This method of control only dictates the position of the backside of the spring and does not force the wearer's ankle to follow any specific or predetermined pattern of motion. This is an important factor and is used to help insure the operator's safety while wearing the actuated device.

In our able-bodied testing, this control approach has worked remarkably well. The device wearer seems to naturally take advantage of the spring's aid and thus shares the walking workload. While walking on a treadmill and utilizing the device for several minutes, the

device wearers' have commented that they do not really feel its aid. However, once the device is removed it takes several awkward steps to resume a natural, un-assisted pattern of gait. As seen previously in Section 4.3, data collected from the actuator device confirms that sharing of walking effort exists.

8. Conclusions

Adaptation of powered actuated devices to assist elderly or weak individuals implies special design requirements. These actuators must be powerful enough to perform the tasks required of them yet remain efficient, lightweight and safe to its wearer. A spring-based actuator can contribute to all of these things.

Springs are inherently powerful and lightweight. For the examples actuators developed above, the springs have 'power to weight' ratios of approximately 300,000 W/kg. Springs are an efficient form of energy storage. For unstressed spring steel, its efficiency is reported to be 99.9% (Carlson, 1980). Springs are by nature compliant and back drivable, thus providing a natural measure of safety. Additionally, the other mechanical actuator elements, like a lead screw, can be designed to promote these design requirements as well (Hollander and Sugar, 2006a).

Methods that include the implementation of springs into wearable system designs are necessary to meet these special design requirements. The development presented here offers a robust approach to the design of actuators that fit a variety of powered assistance situations. The creation of lightweight and practical, powered assistance actuators is possible with today's technology. The era of robots serving a role in everyday life is close at hand and will likely be in the form of powered wearable assistance.

9. References

- ACSM. (1995). ACSM position stand on osteoporosis and exercise, *Medicine And Science In Sports And Exercise*, Vol. 27, No. 4, i-vii
- Blaya, J. & Herr, H. (2004). Adaptive control of a variable-impedance ankle-foot orthosis to assist drop-foot gait, *IEEE Transactions on Neural Systems and Rehabilitation Engineering*, Vol. 12, No. 1, 24-31
- Carlson, H. (1980). *Springs troubleshooting and failure analysis*, 1st ed., Marcel Dekker, Inc., New York
- DeVita, P. & Hortobagyi, T. (2000). Age causes a redistribution of joint torques and powers during gait, *Journal of Applied Physiology*, Vol. 88, 1804-1811
- Elble, R. (1997). Changes in gait with normal aging, *Gait Disorders of Aging: Falls and Therapeutic Strategies* (Masdeu, Sudarsky, and Wolfson, eds.), Lippincott - Raven, Philadelphia, 93-105
- Hof, A.; Elzinga, H.; Grimmius, W. & Halbertsma, J. (2002). Speed dependence of averaged EMG profiles in walking, *Gait and Posture*, Vol. 16, 78-86
- Hollander, K. & Sugar, T. (2004). Concepts for compliant actuation in wearable robotic systems, *Proceedings of the US-Korea Conference (UKC) CDROM*, Research Triangle Park, North Carolina, August 2004
- Hollander, K. & Sugar, T. (2006a). Design of lightweight lead screw actuators for wearable robotic applications, *ASME Journal of Mechanical Design*, Vol. 128, No. 3, 644-648
- Hollander, K.; Ilg, R.; Sugar, T. & Herring, D. (2006b). An efficient robotic tendon for gait assistance, *ASME Journal of Biomechanical Engineering*, Vol. 128, No. 5, 788-791

- Hurst, J.; Chestnutt, J. & Rizzi, A. (2004). An actuator with physically variable stiffness for highly dynamic legged locomotion, *IEEE International Conference on Robotics & Automation (ICRA)*, New Orleans, LA, April 2004
- Kawamoto, H. & Sankai, Y. (2002). Comfortable power assist control method for walking aid by HAL-3, *IEEE International Conference on Systems, Man and Cybernetics*, Vol. 4, pp. 6-11, Hammamet, Tunisia, October 2002
- Kawamoto, H.; Kanbe, S. & Sankai, Y. (2003). Power assist method for HAL-3 estimating operator's intention based on motion information, *IEEE International Workshop on Robot and Human Interactive Communication*, pp. 67-72, Millbrae, CA, October 2003
- Kazerooni, H.; Steger, R. & Huang, L. (2006). Hybrid control of the Berkeley lower extremity exoskeleton (BLEEX), *The International Journal of Robotics Research*, Vol. 25, 561-573
- Nutt, J.; Marsden, C. & Thompson, P. (1993). Human walking and higher-level gait disorders, particularly in the elderly, *Neurology*, Vol. 43, 268-279
- Pratt, J.; Krupp, B.; Morse, C. & Collins, S. (2004). The RoboKnee: An exoskeleton for enhancing strength and endurance during walking, *IEEE International Conference on Robotics and Automation (ICRA)*, pp. 2430-2435, New Orleans, LA, April 2004
- Raibert, M. (1986). *Legged Robots that Balance*, The MIT Press, Cambridge
- Robinson, D.; Pratt, J.; Paluska, D. & Pratt, G. (1999). Series elastic actuator development for a biomimetic walking robot, *IEEE/ASME International Conference on Advanced Intelligent Mechatronics*, pp. 561-568, Atlanta, GA, September 1999
- Rubenstein, L. & Trueblood, P. (2004). Gait and balance assessment in older persons, *Annals of Long-Term Care*, Vol. 12, No. 2, 39-45
- Sugar, T. (2002). A novel selective compliant actuator, *Mechatronics*, Vol. 12, No. 9-10, 1157-1171
- Sugar, T. & Kumar, V. (1998) Design and control of a compliant parallel manipulator for a mobile platform, *ASME Design Engineering Technical Conferences and Computers in Engineering Conference (DETC)*, CDROM, Atlanta, GA, September 1998
- Van Den Bogert, A. (2003). Exotendons for assistance of human locomotion, *BioMedical Engineering Online*, Vol. 2, 17
- Whittle, M. (1996). *Gait analysis: an introduction*, 2nd ed., Butterworth-Heinemann, Oxford
- Winter, D. (1991) *The biomechanics and motor control of human gait: normal, elderly and pathological*, 2nd ed., Waterloo Biomechanics, Waterloo



Rehabilitation Robotics

Edited by Sashi S Kommu

ISBN 978-3-902613-04-2

Hard cover, 648 pages

Publisher I-Tech Education and Publishing

Published online 01, August, 2007

Published in print edition August, 2007

The coupling of several areas of the medical field with recent advances in robotic systems has seen a paradigm shift in our approach to selected sectors of medical care, especially over the last decade. Rehabilitation medicine is one such area. The development of advanced robotic systems has ushered with it an exponential number of trials and experiments aimed at optimising restoration of quality of life to those who are physically debilitated. Despite these developments, there remains a paucity in the presentation of these advances in the form of a comprehensive tool. This book was written to present the most recent advances in rehabilitation robotics known to date from the perspective of some of the leading experts in the field and presents an interesting array of developments put into 33 comprehensive chapters. The chapters are presented in a way that the reader will get a seamless impression of the current concepts of optimal modes of both experimental and applicable roles of robotic devices.

How to reference

In order to correctly reference this scholarly work, feel free to copy and paste the following:

Kevin W. Hollander and Thomas G. Sugar (2007). Powered Human Gait Assistance, Rehabilitation Robotics, Sashi S Kommu (Ed.), ISBN: 978-3-902613-04-2, InTech, Available from:
http://www.intechopen.com/books/rehabilitation_robotics/powered_human_gait_assistance

INTECH
open science | open minds

InTech Europe

University Campus STeP Ri
Slavka Krautzeka 83/A
51000 Rijeka, Croatia
Phone: +385 (51) 770 447
Fax: +385 (51) 686 166
www.intechopen.com

InTech China

Unit 405, Office Block, Hotel Equatorial Shanghai
No.65, Yan An Road (West), Shanghai, 200040, China
中国上海市延安西路65号上海国际贵都大饭店办公楼405单元
Phone: +86-21-62489820
Fax: +86-21-62489821

© 2007 The Author(s). Licensee IntechOpen. This chapter is distributed under the terms of the [Creative Commons Attribution-NonCommercial-ShareAlike-3.0 License](https://creativecommons.org/licenses/by-nc-sa/3.0/), which permits use, distribution and reproduction for non-commercial purposes, provided the original is properly cited and derivative works building on this content are distributed under the same license.

IntechOpen

IntechOpen